

Observations of fronts in the North Sea

by H. M. van Aken,^{1,2} G. J. F. van Heijst¹ and L. R. M. Maas^{1,2}

ABSTRACT

The persistent presence of a cold bottom layer and associated bottom fronts was observed in the stratified central North Sea during an observational program in 1981 and 1982. Moored instruments, capturing a snap-shot of such a front while it was advected past these moorings, revealed the simultaneous presence of a well-defined frontal jet with velocities up to 15 cm s^{-1} . The Coriolis force acting on this jet appeared to be in geostrophic balance with the locally intense pressure gradient forces. Hydrographic surveys revealed the presence of both small-scale and large-scale baroclinic waves on this front, the latter reaching wavelengths of 5–10 internal Rossby radii. Some evidence for a weak secondary circulation in the cross-frontal plane was obtained from the observed deformation of isolines near the front.

1. Introduction

A common feature of continental shelf seas is the general occurrence of strong tidal motions, which induce intense turbulent stirring. In large areas this tidal stirring is so vigorous that it mixes downward any seasonal buoyancy input at the surface, thus preventing the formation of (seasonal) stratification. On the other hand, in areas where the tidal stirring is too weak to keep the water column mixed, thermal stratification can be observed during the spring and summer seasons, when the upper layer is heated due to enhanced insolation. The transition between stratified and vertically mixed regions is usually confined to a narrow zone, generally referred to as 'tidal mixing front'. Most fronts are persistent, and their approximate location can be predicted quantitatively by an energy criterion due to Simpson and Hunter (1974), although advection of a fresher surface layer may complicate this scheme (van Aken, 1986). For most circulation models of the North Sea the fronts and frontal eddies are sub-grid scale phenomena. A better understanding of the properties and the dynamics of these phenomena may lead to a more firmly founded parameterization of these small-scale processes.

Due to their large horizontal dimension, the basic dynamical balance of tidal mixing fronts is in first approximation geostrophic, the pressure gradient force being balanced by the Coriolis force. As a result of the local density distribution, considerable along-frontal velocities will therefore occur in the frontal zone; besides, the flow can be

1. University of Utrecht, Institute of Meteorology and Oceanography, Princetonplein 5, Utrecht, The Netherlands.

2. Present address: Netherlands Institute for Sea Research (NIOZ), Texel, The Netherlands.

expected to exhibit large horizontal and vertical gradients. This along-frontal flow structure has been investigated numerically by James (1978, 1984), and semi-analytically—by using a three-layer geostrophic adjustment model—by van Heijst (1985). James' studies considered the flow in a number of frontal geometries with a continuous—rather than a discrete—stratification. For the tidal mixing front his results revealed the occurrence of an intense jet flow in along-frontal direction, with velocities of the order $10\text{--}15\text{ cm s}^{-1}$. Although velocities of this magnitude have been observed in frontal zones (see e.g. Simpson and Pingree, 1978), observation of a well-defined jet structure near a continental shelf front seems not to have been reported thus far.

In addition to the geostrophically-controlled along-frontal flow there is a weaker, secondary circulation in the cross-frontal plane, mainly caused by frictional processes. This secondary circulation has been examined in the cited numerical studies of James (1978, 1984), and also in a semi-analytical way by Garrett and Loder (1981). It was found that—for tidal mixing fronts—the cross-frontal circulation has a two-cell pattern, with an upwelling flow on the mixed side of the front. An interesting feature of the secondary flow structure is a region of convergence at the sea surface. Because the velocities associated with the cross-frontal flow are extremely small, direct measurement is impossible. However, observations have provided indirect evidence for the existence of a two-cell circulation pattern: the frequent occurrence of a narrow band of lower sea-surface temperatures on the mixed side of the front (see e.g. Simpson *et al.*, 1978; Krause *et al.*, 1986) indicates the presence of an upwelling flow, and the frequently observed accumulation of floating material in the frontal zone implies surface convergence.

In general, a front acts as a physical boundary between water masses of different thermal and saline structure. Because the cross-frontal fluxes of properties are locally intense, frontal zones create favorable conditions for a variety of biological processes. This exchange of properties is believed to play a crucial role with respect to the primary production and the associated enhanced biological activity, as often observed near fronts (see e.g. Bowman and Esaias, 1978).

Observation by satellites has provided evidence that surface fronts are unstable, as can be concluded from the abundance of meanders and vortex-like flow structures in frontal regions (see e.g. Pingree, 1978, 1979). Apart from theoretical studies, the instability behavior of surface and bottom fronts has been examined in the laboratory by Griffiths and Linden (1981, 1982) and by van Heijst (1986), respectively. This experimental work has provided important information about the evolution of the unstable front and the subsequent formation of frontal eddies. James (1984) has studied the instability behavior numerically, and his results show good agreement with both the laboratory observations mentioned above and the available sea-surface observations with regard to the most unstable wavelength.

It is well known, see e.g. Tomczak and Goedecke (1964), that in the North Sea the

region southeast of the Dogger Bank is seasonally stratified. As part of a larger joint-project with the KNMI (De Bilt) and the NIOZ (Texel) observations were carried out near the southern edge of this seasonally stratified area during the spring, summer and autumn seasons of 1981 and 1982. The observations were done by CTD measurements along systematic tracks, as well as by use of current meters and thermistor chains that were moored near the frontal zone. In this way some valuable information about the frontal dynamics was collected, which will be presented in this paper.

In particular, the current meter recordings revealed the existence of a *frontal jet* with a velocity magnitude of approximately 15 cm s^{-1} . This jet-like flow was recorded at the simultaneous passage of the frontal zone, as revealed by the temperature and salinity measurements. Another important result was obtained from the thermistor recordings, by which the cross-sectional thermal structure of the (slowly advecting) front could be reconstructed. The shape of the isotherms revealed a characteristic downward *dip* at some distance from the bottom front—a feature believed to be caused by a downwelling flow in the cross-frontal circulation.

The paper is organized as follows—the hydrography of the research area as well as data obtained by a number of large-scale and small-scale surveys are presented in Section 2. Then, Section 3 focusses on the observations by instruments that were moored in the frontal zone; it describes the thermistor data from which the temporal development of the front was deduced and also the current meter data which revealed the existence of the along-frontal jet. Finally, the presented observations are discussed more generally in Section 4.

2. Hydrography of the research area

During the spring, summer and autumn seasons of 1981 and 1982 observations were carried out, in cooperation with the Dutch institutes KNMI (De Bilt) and NIOZ (Texel), in the North Sea area between $53^{\circ}30'N$ and $55^{\circ}30'N$, and $2^{\circ}30'E$ and $5^{\circ}30'E$. Current meters and thermistor chains were moored in the central part of the research region (see Fig. 1). Details of the moored instruments are summarized in Table 1. Salinity and temperature were measured by CTD recordings at a number of stations situated at a regular distance of 8 nautical miles along systematic tracks (large-scale surveys). In the central part of the research area additional CTD surveys were carried out with a distance between successive stations of 2 miles (small-scale surveys). Locally, the bottom topography can be characterized as a bowl shape, with the observation point A ($54^{\circ}30'N$, $4^{\circ}30'E$) roughly located in the bowl center, where the sea depth measures almost 50 m. The topography is rather smooth, and in particular in SSE direction the bottom slopes upward very gently, into the mixed area north of the Dutch Wadden Isles.

According to Tomczak and Goedecke (1964) the central part of the area of interest

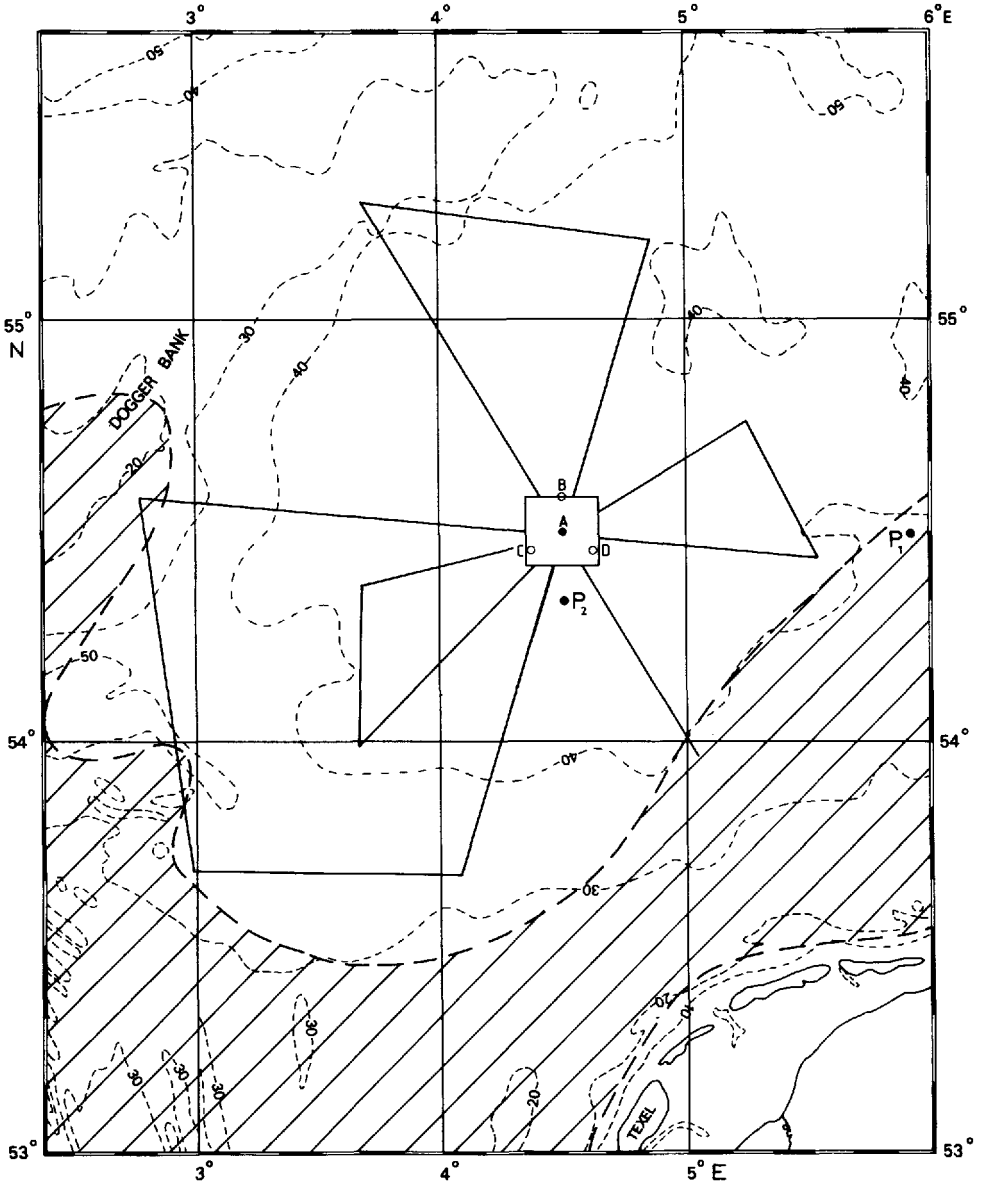


Figure 1. Schematic map of the research area. Depth contours are denoted by broken lines; the number in each contour indicates the depth in meters. The hatched area represents the transition zone between stratified and well-mixed parts of the sea (according to Pingree, 1978). Large-scale CTD surveys were carried out in 1982 along the tracks indicated by full lines. Current meters and thermistor chains were moored at the positions A, B, C and D. The bottom pressure was recorded at positions P_1 and P_2 . A large number of small-scale CTD-surveys was carried out in the square area centered in A.

Table 1. Positions of the moored instruments as described in this study. Further details of the moorings and the other instruments used in the 1981 and 1982 observational programs are given by Maas and van Haren (1986).

	N	E	Instruments
A	54°30'	4°30'	current meters (81–82), thermistor chain (81–82)
B	54°30'	4°30'	current meters (81–82)
C	54°27'	4°22'	current meters (81–82), thermistor chain (82)
D	54°27'	4°28'	current meters (81–82), thermistor chain (82)
P ₁	54°30'	5°54'	pressure gauge (82)
P ₂	54°20'	4°30'	pressure gauge (82)

is thermally stratified in summer. The transition zone between seasonally stratified and mixed parts of the southern North Sea is represented by the hatched band in Figure 1.

For the period of well-established stratification a typical example of the large-scale horizontal distribution of temperature and salinity as measured near the sea bottom is given in Figure 2. The distributions shown in these graphs are based on the large-scale survey made during the period from day 227 to day 230 (15 to 18 August) in 1982. An east-west section of temperature and salinity distributions as observed during this survey is shown in Figure 3. The temperature section clearly shows that most of the isotherms bend downward, terminating on the bottom rather than at the sea surface. Similar thermal structures were observed along other tracks, at different times in the stratified season. From these observations it is obvious that the surface temperature hardly indicates any frontal structure. And indeed, thermal fronts as transition zones between stratified and mixed areas in this part of the North Sea can only rarely be observed by infrared satellite imagery. This is in marked contrast with the fronts as occurring in the Celtic Sea and in the Irish Sea, where pronounced thermal surface fronts can be observed regularly (see e.g. Simpson and Pingree, 1978). Nevertheless, though a sharp (thermal) transition between stratified and well-mixed areas is not visible at the sea surface, sharp fronts might occur at greater depths, e.g. near the sea bottom. Such fronts should then be visible in the bottom temperature distribution as shown in Figure 2c. However, the horizontal resolution of the large-scale surveys was limited by the station distance (8 miles), so that sharp fronts will be smoothed in the analysis of the observational data. During the large-scale surveys the east-west bottom temperature gradient $\Delta T_b/\Delta x$ (T_b being the bottom temperature, and x the coordinate in eastward direction) measured approximately $6.2 \times 10^{-5} \text{ }^\circ\text{C m}^{-1}$ in the proximity of the moored instruments. The small-scale surveys performed in the week prior to the large-scale survey of Figure 2, with station distances of 2 miles, showed considerable variation in $\Delta T_b/\Delta x$, as illustrated in Figure 4, although the mean value of the bottom temperature gradient according to the small-scale surveys measured $6.0 \times 10^{-5} \text{ }^\circ\text{C m}^{-1}$. This variation indicates the possible presence of small-scale bottom fronts with a

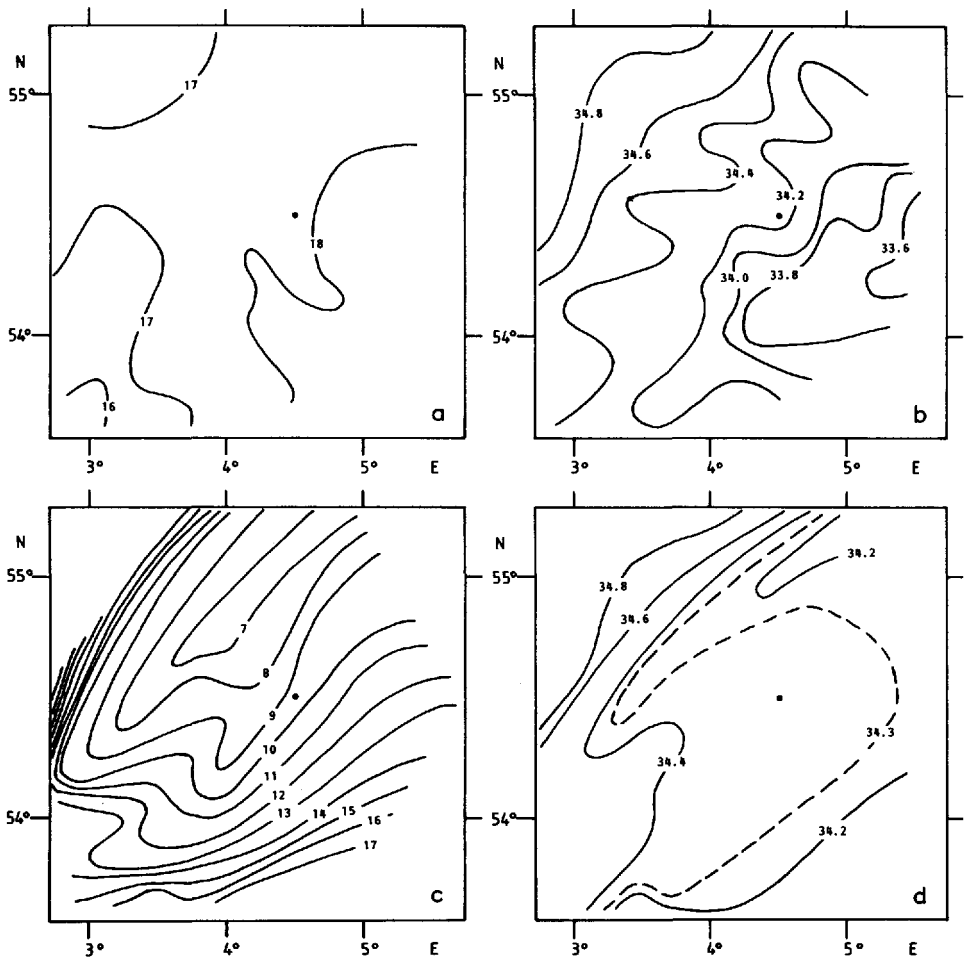


Figure 2. Horizontal distributions of temperature and salinity as observed during the large-scale CTD survey carried out in the period day 227–day 230 in 1982. The graphs represent (a) the sea-surface temperature ($^{\circ}\text{C}$), (b) the sea-surface salinity (pss-78), (c) the near-bottom temperature ($^{\circ}\text{C}$), and (d) the near-bottom salinity (pss-78). The black dot indicates the central position A as shown in Figure 1.

width of distinctly less than 8 miles, probably of about 2 miles or 4 km. This value of 4 km happens to correspond to the order of the internal Rossby radius of deformation as defined by Griffiths and Linden (1982). The strong variation of the horizontal temperature gradient as displayed in Figure 4 is likely to be caused by small-scale baroclinic eddy motion, leading to small-scale frontogenesis.

However, eddies may have much larger scales, as can for example be seen from Figure 5, which presents the horizontal distribution of the bottom temperature as

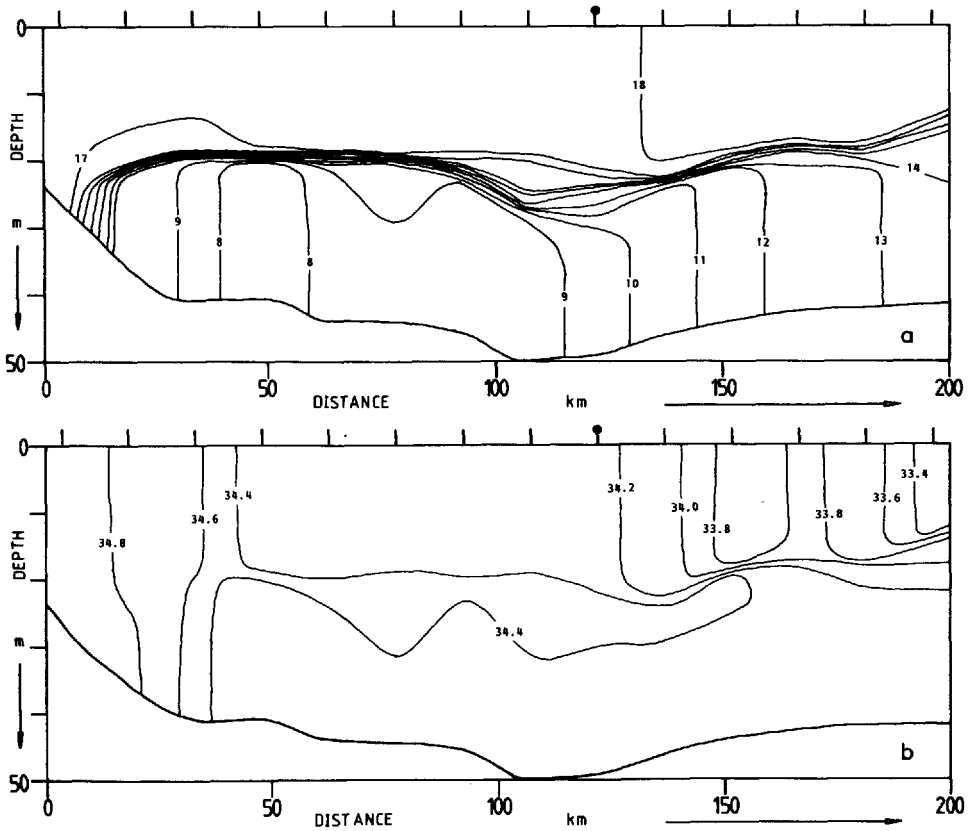


Figure 3. Vertical distributions of (a) temperature ($^{\circ}\text{C}$) and (b) salinity (pss-78) along the west-east section of the large-scale CTD survey carried out in the period day 227–day 230 in 1982. The dashes on the upper side of each section indicate the CTD stations; the black dot denotes the central position A as shown in Figure 1.

observed during a large-scale survey made in the period from day 260 to 262 (17–19 September) in 1982. Comparison with the bottom temperature structure as observed in the earlier survey (Fig. 2c) makes clear that within one month large waves have grown in the temperature field, with wavelengths of typically 40 km and amplitudes of roughly 20 km. Similar meanders have been observed during other surveys, both in 1981 and 1982, and occasionally eddies were encountered that were pinched off from the main cold core. The wavelength of the meanders in the bottom layer appeared to be approximately 10 times the internal Rossby scale of deformation, as used by Griffiths and Linden (1982). This value agrees with the laboratory observations of unstable bottom fronts as reported by van Heijst (1986).

The structure of a single eddy in the bottom layer was examined in more detail during an extended small-scale survey made in the period from day 219 to 221 in 1981.

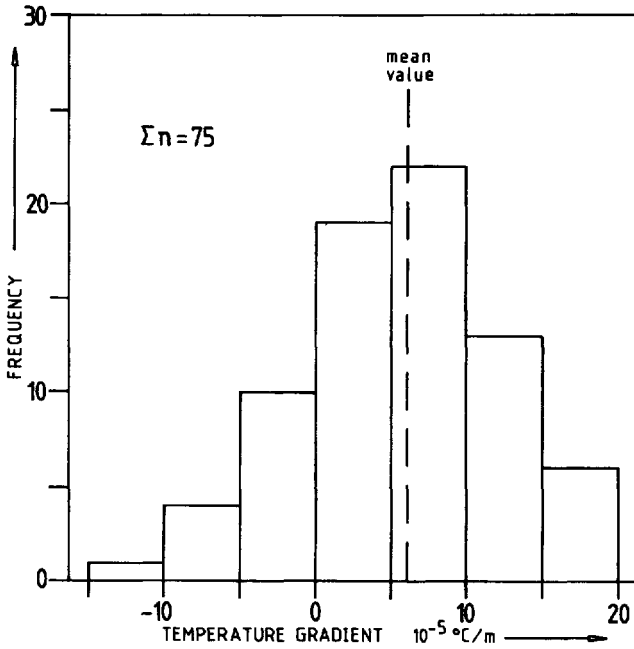


Figure 4. The frequency distribution of the east component of the horizontal near-bottom temperature gradient derived from the small-scale CTD surveys carried out in the period day 220–day 226, 1982. The station spacing was 2 nautical miles.

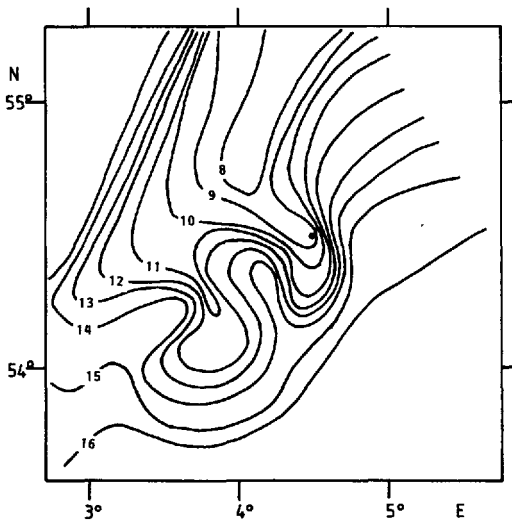


Figure 5. Horizontal distribution of the near-bottom temperature ($^{\circ}\text{C}$) as observed during the large-scale CTD survey carried out in the period day 260–day 262, 1982. The black dot indicates the central position A.

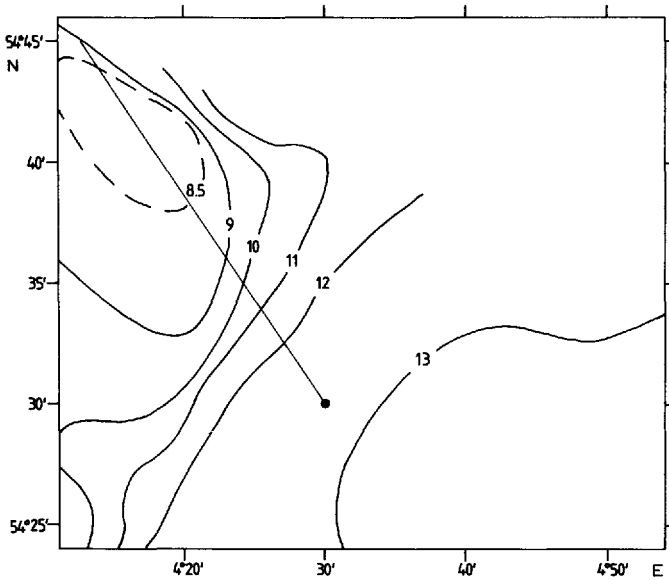


Figure 6. Horizontal distribution of the temperature ($^{\circ}\text{C}$) at a depth of 42.5 m as observed during the extended small-scale survey carried out in the period day 219–day 221, 1981. The black dot indicates the central position A.

This survey was performed in a $40\text{ km} \times 40\text{ km}$ area with distances of 2 miles between successive stations. The observed horizontal distribution of the bottom temperature is shown in Figure 6. The salinity distribution has a similar shape, but because of its minor dynamical importance it is not presented here. The core of the meander, characterized by lower temperatures, lies in the NW part of the survey area. This cold core was surrounded by a rather well-defined front in which the horizontal temperature gradient increased locally to values close to $10^{-3}\text{ }^{\circ}\text{C m}^{-1}$. One of the tracks of the small-scale survey runs approximately in NNW direction just through the center of the cold meander core, as indicated in Figure 6. The vertical distributions of temperature, salinity and density as measured along this track are presented in Figure 7.

It is obvious from the resemblance between the temperature and density sections that the density structure is mainly determined by the thermal field, rather than by the salinity distribution. The graphs show a well-defined bottom front (a temperature jump of 3.5°C within 8 miles), with a characteristic 'doming' of the isotherms and the isopycnals (Figure 7, around $x = 24\text{ km}$) before they terminate onto the sea bottom. This doming of the isotherms close to the bottom front was also observed in the other surveys, carried out in the periods May–September in 1981 and 1982. Most likely it is caused by the weak circulation in the cross-frontal plane, also found in the numerical simulations by James (1984). Similar evidence was obtained recently by Pollard (1986) from observation of an oceanic surface front. According to Figure 7a,b, the

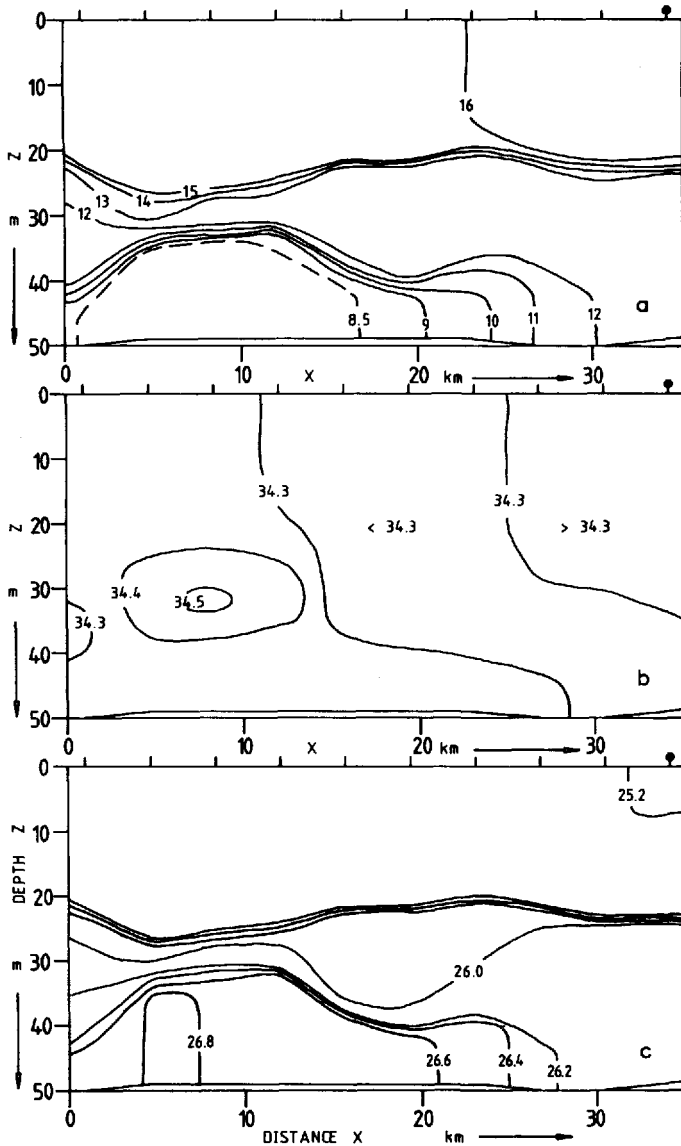


Figure 7. Vertical distributions of (a) temperature ($^{\circ}\text{C}$), (b) salinity (pss-78), and (c) density excess (kg m^{-3}) along the section indicated in Figure 6, as observed during the extended small-scale survey carried out in the period day 219–day 221, 1981. The dashes on the upper side of the sections indicate the CTD stations; the black dot indicates the central position A.

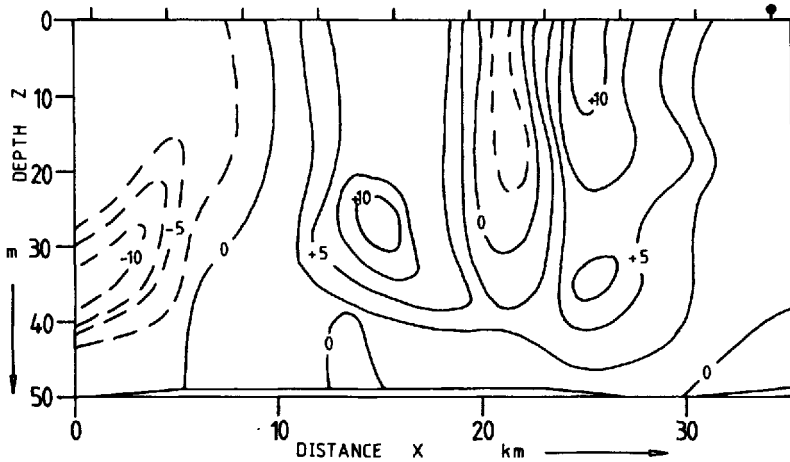


Figure 8. Vertical distribution of the cross-sectional geostrophic velocity (cm s^{-1}), calculated from the sections displayed in Figure 7. The reference level was taken at the bottom. Positive velocities are directed toward ENE. The dashes indicate the CTD stations, and the black dot indicates the central position A.

upper 20 m of the water column seems to be well mixed, and no surface front is visible. The thermocline between the wind-mixed upper layer and the lower parts of the water column is well developed, and appears to extend from the cold meander core into the outer region, only showing a slight upward doming just above the bottom front. As before, this doming can be explained from the secondary circulation, as modelled by James (1984). The isotherms defining the bottom front indicate the presence of a second thermocline at some distance from the front. This lower thermocline separates the cold meander core from warmer water intruding from outside the frontal zone. Over the center of the cold core this intrusion has a thickness of only a few meters, while its thickness increases to about 20 m at the position of the bottom front. Over the cold core ($x = 0 - 20$ km) the depths of both thermoclines change in a reciprocal way. The resulting wedge-shaped intrusion of warmer bottom water, also clearly visible in the density structure, indicates the presence of an intermediate baroclinic velocity maximum, similar to the situation discussed theoretically by van Heijst (1985).

The graphs shown in Figure 7 may serve as *typical* examples of the distribution of physical properties: similar distributions have been observed during various small-scale surveys in the frontal zone, both in 1981 and 1982. The inference to be drawn is that, if density fields like the one displayed in Figure 7 are geostrophically balanced—which their persistent nature leads us to believe—we may expect them to be accompanied by strong spatially varying baroclinic current fields. This is indeed what can be observed in Figure 8, representing the *calculated* geostrophic current field corresponding to the density distribution shown in Figure 7c. For the calculations the level of no motion was set at the sea bottom. It is reasonable to assume—at least on this horizontal scale,

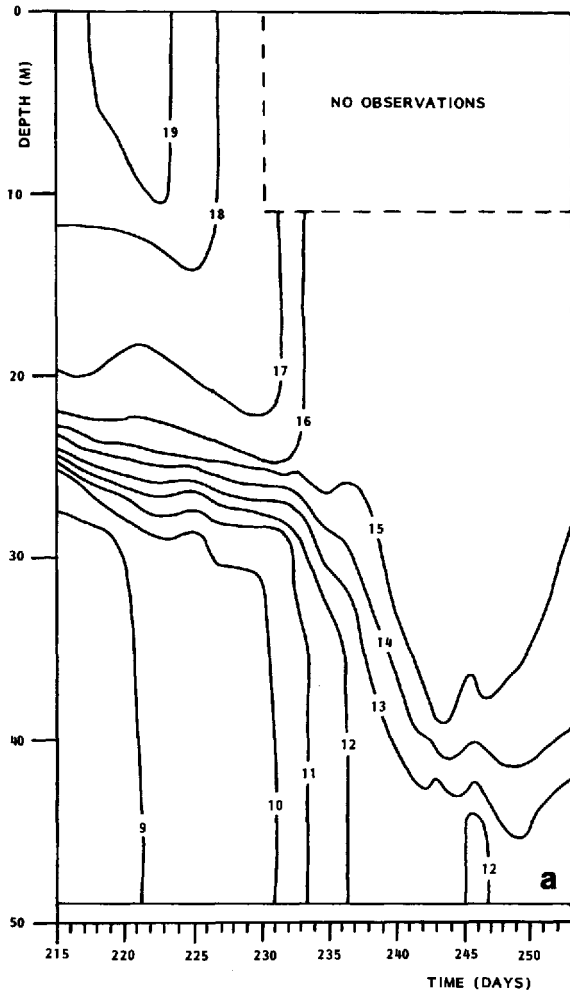


Figure 9. Temporal sections of low-pass filtered temperature and velocity as observed at the central position A during the summer of 1982: (a) section of the temperature ($^{\circ}\text{C}$), and (b) section of the velocity component (cm s^{-1}) in the direction 33° true north. The temperature data were obtained from the thermistor chain, the thermistors mounted at the current meters, and from the CTD surveys carried out in that period. The current meter depths are indicated by arrow heads.

which is based on station distances of roughly one internal Rossby radius—that the calculated geostrophic current is a reliable estimate of the baroclinic part of the flow. Figure 8 reveals the existence of a baroclinic geostrophic jet at mid-depth with velocities larger than 10 cm s^{-1} . This jet is directly related to the wedge of intruding warmer bottom water mentioned above, and it appears to circumvent the thermocline water above the cold core which has clearly different salinity characteristics (see

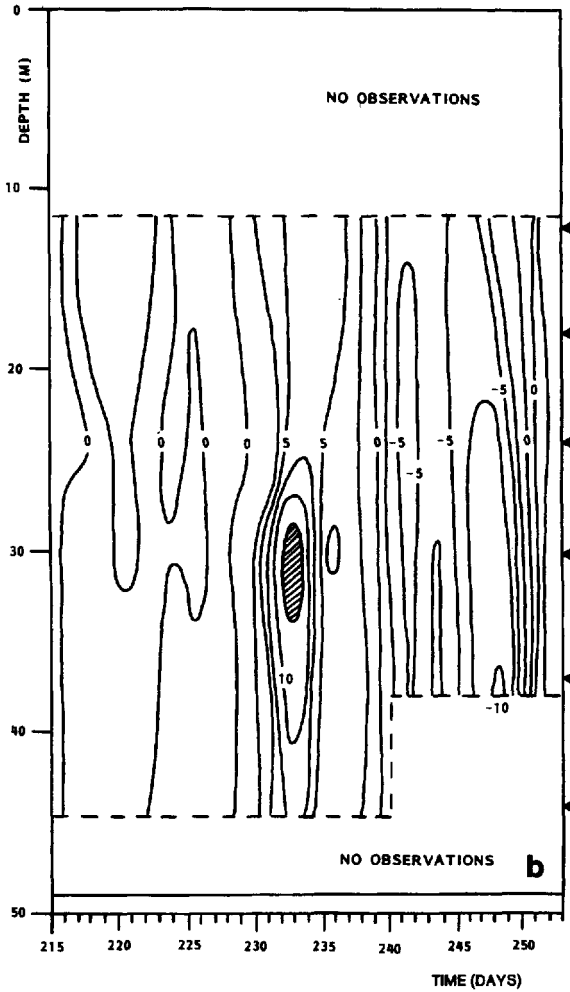


Figure 9. (Continued)

Fig. 7b). CTD sections in other directions through the meander revealed that such an intermediate baroclinic jet is present all around the core of the meander. In the next section a comparison between the calculated geostrophic velocities and data obtained from current meter recordings will be made.

3. Observation by moored instruments

Apart from CTD observations during large-scale and small-scale surveys, important information about the stratification structure was also obtained from the thermistor chains and current meters that were moored at the stations A, B, C and D (see Fig. 1). The positions of the moored instruments are presented in Table 1.

During the late summer of 1982 it was observed that the bottom front moved slowly in a northwestern direction, such that the thermistors and the current meters originally located on the stratified side of the front were able to measure the temperature distribution and the flow structure in a frontal cross-section. In order to eliminate diurnal and higher frequencies, the time dependent thermistor and current meter signals were low-pass filtered, and characteristic graphs of the data obtained at position A are shown in Figure 9. In these graphs the parameters along the abscissa and the ordinate are time (in Julian days) and depth (in meters). The isotherms (Fig. 9a) are plotted for differential temperatures of 1°C , ranging from 9°C near the bottom to 19°C in the upper parts of the water column. Up to day 230 the temperature graph clearly indicates the presence of a well-defined thermocline on the cold side of the bottom front at roughly 20–25 m depth, with a large drop from 16°C to 10°C over a few meters depth.

Since the data displayed in Figure 9a might very well be affected by local changes due to wind and tidal mixing as well as by changes due to advection, interpretation of the data is difficult without having additional information about these effects. Increased mixing due to strong wind events usually occurs on a time scale small compared to the characteristic time scale associated with tidally-driven mixing (see e.g. van Aken, 1984). In order to estimate the relative importance of the mixing by atmospheric forcing, we used the wind data from weather maps published daily by the Deutsche Wetterdienst. These showed that up to day 223 the weather was calm, with wind velocities less than 8 m s^{-1} . After day 223, however, some gales developed with occasional wind velocities over 18 m s^{-1} . These gales obviously caused the cooling and deepening of the surface mixed layer down to a depth of approximately 40 m. During that period the temperature near the bottom increased from less than 9°C to more than 12°C , an effect most likely caused by advection.

From the large-scale and small-scale CTD surveys, and also from the current measurements as shown in Figure 10, it was derived that the front was, during its passage, directed approximately 33 degrees true north. In order to gain some insight in the along-frontal flow structure, the low-pass filtered velocity component in that particular direction is plotted in Figure 9b. An interesting feature of this velocity graph is the *jet-like* flow occurring in the period from 230 to day 235, coinciding exactly with the passage of the front. The presence of this jet was also confirmed by the low-passed current measurements at the positions C and D. Its magnitude is quite considerable, and reaches values up to 15 cm s^{-1} .

Extrapolation of the observed shear to the bottom and to the surface suggests that part of the observed current is barotropic, with velocity magnitudes up to 7 cm s^{-1} during that particular period. This was confirmed by data obtained from a pair of bottom-mounted self-recording pressure transducers. One of these (P_2) was located 10 miles south of the central position A and the other (P_1) 49 miles east of A, such that they were approximately 50 miles apart. Figure 11 shows the signals of these pressure

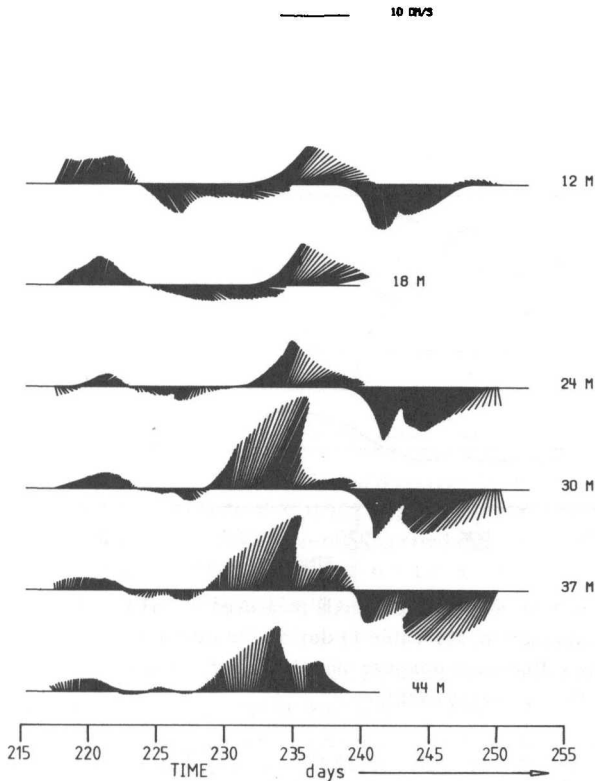


Figure 10. Stick plots of the low-pass filtered velocity vectors observed at position A during the summer of 1982. The observation depths (in m) are indicated on the right.

gauges, which were low-pass filtered and shifted in order to obtain a zero-mean for the period of observation. The lowermost graph in Figure 11 presents the differential pressure signal. Although these pressure signals do not allow calculation of the mean horizontal pressure gradient, they do provide important information about nonstationary events during the observation period. A striking event is visible between day 229 and 235, which shows up as a well-defined bump in the differential pressure curve. This bump is most likely to be associated with a wind-induced slope of the sea surface during one of the strong wind events mentioned above. The change in the geostrophic bottom velocity component in the direction 349° true north, which can be calculated from this horizontal pressure gradient, reaches a value of approximately 6.5 cm s^{-1} . This agrees with the earlier-mentioned magnitude of the barotropic current in that particular period.

Unfortunately, it is not possible to compare the observed shear associated with the frontal jet with the *actual* density distribution, since the CTD surveys were terminated just before the jet was recorded by the moored instruments. For this reason we used the

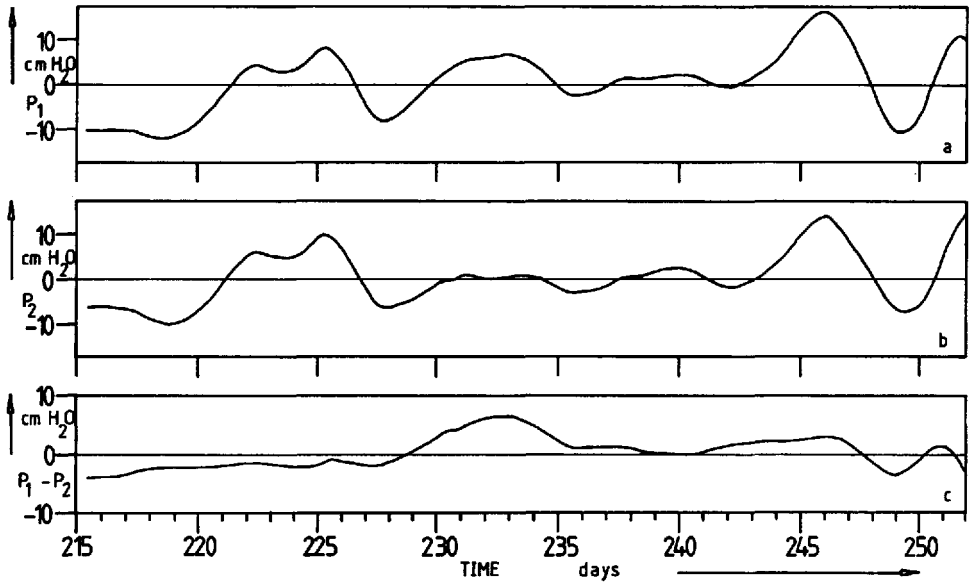


Figure 11. Low-pass filtered pressure signals measured at (a) the position P_1 and at (b) the position P_2 (for explanation, see Table 1) during the summer of 1982. The lowermost graph (c) represents the differential pressure signal $P_1 - P_2$. The pressures are expressed in cm water, and are shifted to a zero average.

most recent information available, being the density distribution as determined during the last small-scale CTD survey on day 226. Two stations were selected at a distance of 4 km apart, with bottom temperatures in the range 9.9°C – 10.4°C , and the associated geostrophic shear in the direction 28° true north was calculated from the density structure. A comparison between this result and the observed five-days mean velocity profile associated with the frontal jet is presented in Figure 12. A shift in the velocity magnitude was required to fit the observed and the calculated profiles, which corresponds with the presence of the earlier-mentioned barotropic current on which the baroclinic jet was superposed. The required velocity shift agrees well with the magnitude of the barotropic flow. Apart from the shift, the observed and the calculated velocity curves show good agreement. The dents in the velocity distributions displayed in Figure 12 are directly associated with the pronounced doming of the pycnocline, which causes the geostrophic shear to change sign locally, more or less in the way as observed in August 1981 (cf. Fig. 8).

In order to analyze the spatial coherence of the frontal passage as observed at position A, it is useful to draw a comparison with the signals recorded simultaneously by instruments moored at the other stations. Figure 13 shows the time-dependent temperature distribution as observed at moorings C and D for the same period as the observations presented in Figure 9. Comparison shows that, apart from some small phase differences, the surface mixed layer is coherent over horizontal distances of

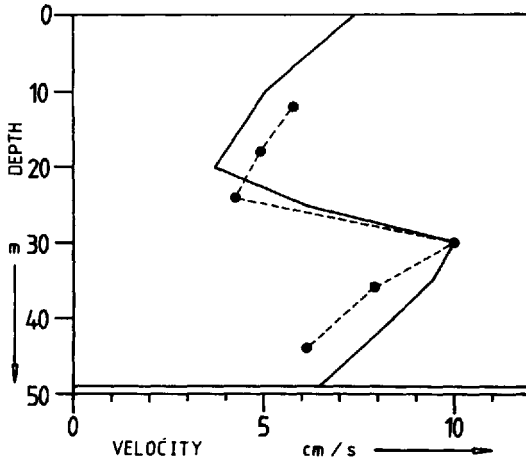


Figure 12. The observed mean velocity (cm s^{-1}) in the direction 033° , measured at the central mooring A during the period day 230–day 235, 1982 (black dots) and the geostrophic velocity computed from a previous small-scale CTD survey, carried out on day 226, 1982. For the geostrophic calculation a near-bottom velocity of 6.5 cm s^{-1} was assumed, which is in accordance with the pressure difference shown in Figure 11.

5 miles, being equivalent to the distance between adjacent mooring positions. However, in the bottom layer the situation is different: variations occur from mooring to mooring, mainly after day 235. In particular the temperature signal recorded at mooring C, SSW of the central position, shows a number of frontal features, likely to be associated with meandering of the bottom front. Also note the downward doming of the 11° – 15° isotherms during days 223–228, again probably due to a downwelling cross-frontal circulation. The currents recorded at the moorings B, C and D are presented in the form of stick plots, as shown in Figure 14. Comparison of these plots with the stick plots corresponding to the central mooring A (Fig. 10) confirms the assumption of a meandering front: while the currents at the positions A and D are directed southward after day 238, the current meter in the bottom layer at B and the meters at all levels at C indicate northward currents until day 245, with a jet-like maximum at a level of 27 m at mooring C. This spatial variability in the current structure has the same character as that observed in the preceding year (cf. Fig. 8), which is attributed to variations in the density distribution.

4. Discussion and conclusions

The results presented in the previous sections clearly show that the fronts observed in the stratified North Sea mainly have the character of bottom fronts, with isotherms terminating on the sea bottom. For this reason the fronts do formally not belong to the class of “tidal mixing fronts,” which are generally defined as the transition zones between (seasonally) stratified areas and fully mixed areas; at such fronts the

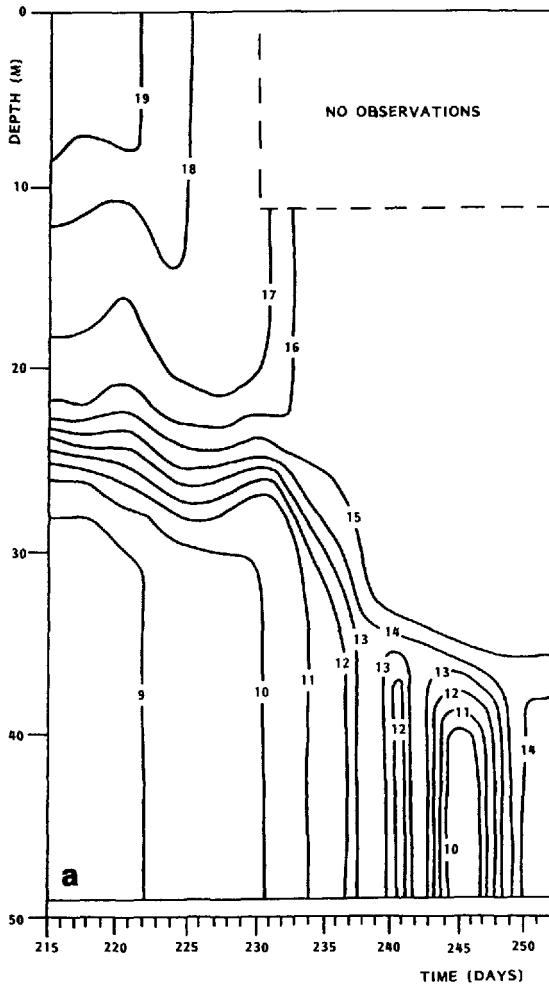


Figure 13. Temporal sections of the low-pass filtered temperature ($^{\circ}\text{C}$) as observed during the summer of 1982 (a) at position C and (b) at position D. The positions are shown in Figure 1.

associated isolines usually have a “forked” appearance, in that some of the lines bend downward and terminate on the bottom, while the other isolines bend upward and terminate at the sea surface. The fronts observed in the stratified southern North Sea, however, can be regarded as transition zones between adjacent areas that are stratified, but at different rates. The reason for this difference lies in the generation of the stratification and its subsequent development as well as in effects due to advection and mixing by wind and tides.

The surface layer of the sea is usually well-mixed by wind, and therefore hardly shows any frontal regions. Because the sea surface temperature appears to be adapted

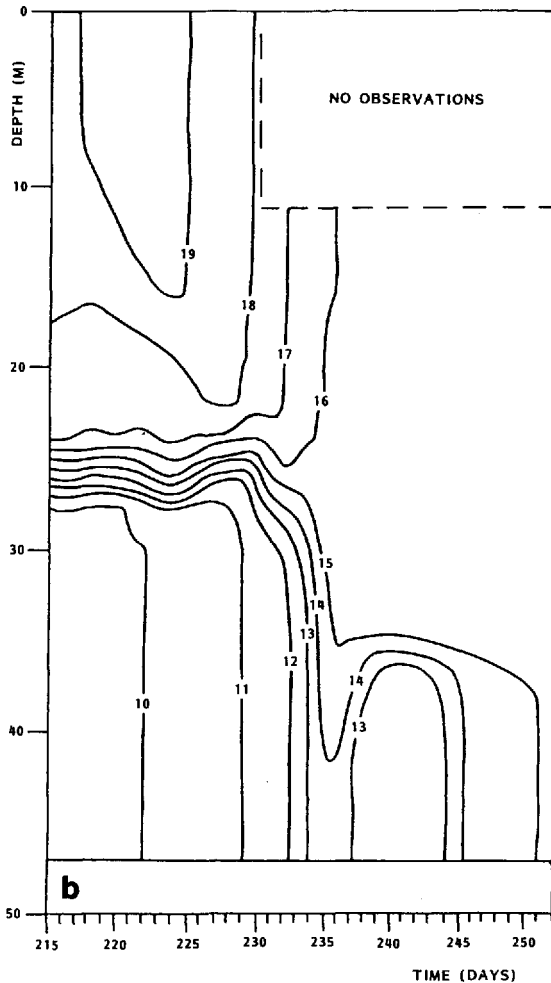


Figure 13. (Continued)

quite fast to the atmospheric forcing, the positions of the fronts in the central North Sea cannot be derived from infrared satellite pictures. The “forked” structure of the isolines seen in Figures 9a and 13 is caused by the nearly simultaneous occurrence of a strong wind mixing event and the passage of the bottom layer front.

On the scale of the central North Sea the (bottom) fronts show meander-like variations, although with varying intensity; this can be clearly seen by comparing Figures 2c and 5. These meanders in the bottom temperature field were observed to have typical dimensions of the order of several times the internal Rossby radius, which agrees with the numerical results obtained by James (1984) and with the laboratory results obtained both by Griffiths and Linden (1982) and by van Heijst (1986). When

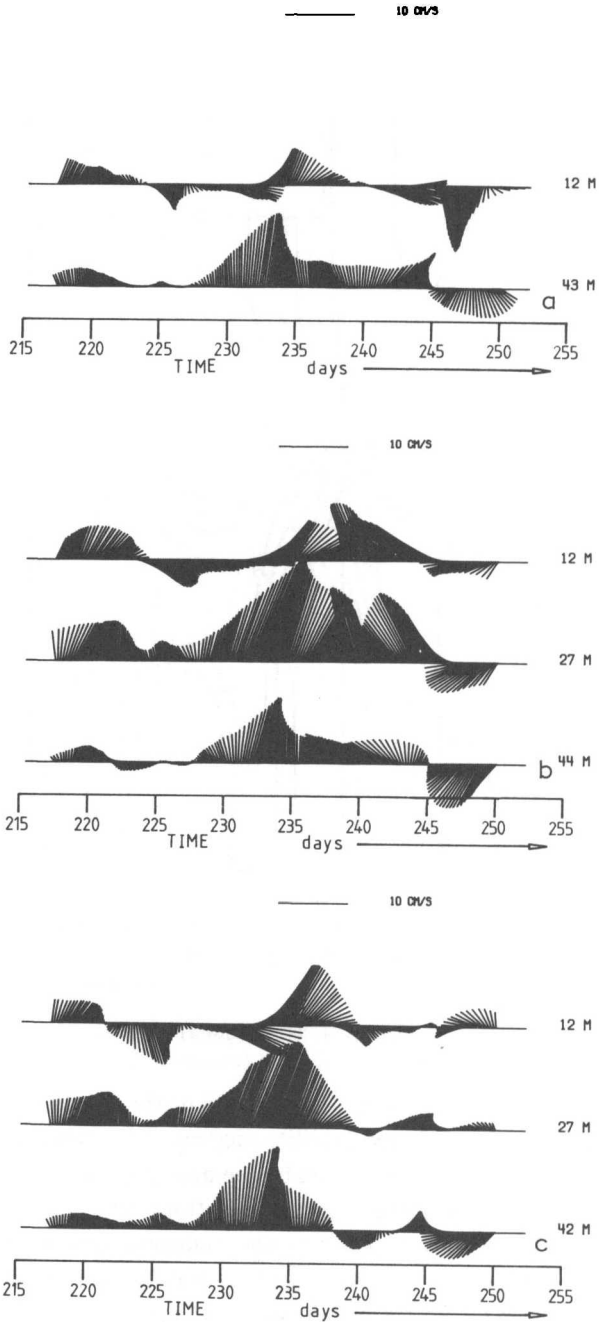


Figure 14. The graphs in (a), (b) and (c) are stick plots of the low-pass filtered velocity vectors observed during the summer of 1982 at the positions B, C and D, respectively, as shown in Figure 1. The observation depths (in m) are indicated on the right.

meanders reach large amplitudes they may be pinched off from the front and thus form isolated cold-core or warm-core eddies, a process that might provide an important mechanism for the cross-frontal transport of properties. For some fixed positions the pronounced frontal meandering was observed to induce variations of several degrees Celsius in the bottom temperature on time scales varying from a few days to a couple of weeks. It can be anticipated that such drastic changes in the hydrographic parameters may cause a serious stress on the bottom fauna.

The width of the bottom fronts was found to be of the order of one internal Rossby deformation radius. Comparison of the observed cross-frontal distributions of temperature and salinity revealed a number of additional characteristic features. One of these is the doming of the isolines at some small distance from the front; this doming is assumed to be due to the weak secondary circulation in the cross-frontal plane, in accordance to the numerical simulations by James (1984). The intrusion of warm bottom water between the surface and bottom mixed layers bears resemblance to the flow studied by van Heijst (1985) in a geostrophic adjustment model of a front. The horizontal density gradients in the frontal zone (including the effects due to the doming of isopycnal surfaces and the presence of wedge-shaped intrusions) imply baroclinic geostrophic flows in the along-frontal direction, which take the appearance of sub-surface jets with velocity magnitudes of more than 10 cm s^{-1} . The horizontal scale of these jets is of the order of 5 to 10 km (see Fig. 8), which is roughly one or two internal Rossby radii. Note that this predicts horizontal shears $O(5 \cdot 10^{-5} \text{ s}^{-1})$, which are an order of magnitude larger than those recently observed in the homogeneous parts of the North Sea (Riepma, 1986). Current meter observations confirm this picture, and the observed vertical shear agrees with the calculated geostrophic shear (see Fig. 12).

In summary, the observations in the central North Sea reveal the presence of strong bottom fronts with associated frontal jets, cross-frontal circulation and low-frequency baroclinic frontal waves, each of which bear their particular impact on the local water properties and associated bio-fauna.

REFERENCES

- Aken, H. M. van. 1984. A one-dimensional mixed layer model for stratified shelf seas with tide- and wind-induced mixing. *Deutsche Hydrographische Zeitschrift*, 37, 3–27.
- 1986. The onset of seasonal stratification in shelf seas due to differential advection in the presence of a salinity gradient. *Cont. Shelf Res.*, 5, 475–485.
- Bowman, M. J. and W. E. Esaias. (eds.). 1978. *Oceanic Fronts in Coastal Processes*. Springer, Berlin, 114 pp.
- Garrett, C. J. R. and J. W. Loder. 1981. Dynamical aspects of shallow sea fronts. *Phil. Trans. Roy. Soc. London*, A302, 563–581.
- Griffiths, R. W. and P. F. Linden. 1981. The stability of buoyancy-driven coastal currents. *Dyn. Atmos. Oceans*, 5, 281–306.
- 1982. Laboratory experiments on fronts. Part 1: Density-driven boundary currents. *Geophys. Astrophys. Fluid Dyn.*, 19, 159–187.
- Heijst, G. J. F. van. 1985. A geostrophic adjustment model of a tidal mixing front. *J. Phys. Oceanogr.*, 15, 1182–1190.

- 1986. On the dynamics of a tidal mixing front, *in* *Marine Interfaces Ecohydrodynamics*, J. C. J. Nihoul, (ed.), Elsevier, Amsterdam, 165–194.
- James, I. D. 1978. A note on the circulation induced by a shallow-sea front. *Estuar. Coastal Mar. Sci.*, *7*, 197–202.
- 1984. A three-dimensional numerical shelf-sea front model with variable eddy viscosity and diffusivity. *Cont. Shelf Res.*, *3*, 69–98.
- Krause, G., G. Budeus, D. Gerdes, K. Schaumann and K. Hesse. 1986. Frontal systems in the German Bight and their physical and biological effects, *in* *Marine Interfaces Ecohydrodynamics*, J. C. J. Nihoul, (ed.), Elsevier, Amsterdam, 119–140.
- Maas, L. and H. van Haren. 1986. Data report of current, temperature and pressure observations in the stratified central North Sea, 1980–1982. IMOU Report R-86-14, University of Utrecht, 96 pp.
- Pingree, R. D. 1978. Cyclonic eddies and cross-frontal mixing. *J. Mar. Biol. Ass. U.K.*, *58*, 955–963.
- 1979. Baroclinic eddies bordering the Celtic Sea in late summer. *J. Mar. Biol. Ass. U.K.*, *59*, 689–698.
- Pollard, R. T. 1986. Frontal surveys with a towed profiling conductivity/temperature/depth measurement package (*SeaSoar*). *Nature*, *323*, 433–435.
- Riepma, H. W. 1986. Note on observed vorticity of residual currents in an area of the Southern Bight of the North Sea. *Deutsche Hydrographische Zeitschrift*, *39*, 161–167.
- Simpson, J. H., C. M. Allen and N. C. G. Morris. 1978. Fronts on the Continental Shelf. *J. Geophys. Res.*, *83*, 4607–4614.
- Simpson, J. H. and J. R. Hunter. 1974. Fronts in the Irish Sea. *Nature*, *250*, 404–406.
- Simpson, J. H. and R. D. Pingree. 1978. Shallow sea fronts produced by tidal stirring, *in* *Oceanic Fronts in Coastal Processes*, M. J. Bowman and W. E. Esaias, (eds.), Springer, Berlin, 29–42.
- Tomczak, G. and E. Goedecke. 1964. Die thermische Schichtung der Nordsee. *Deutsche Hydrographische Zeitschrift, Ergänzungsheft Reihe B(4)*, Nr. 8, 182 pp.